Measurement of the neutron fraction event-by-event in DREAM

John Hauptman, for the DREAM Collaboration[1]

Department of Physics and Astronomy, Iowa State University, Ames, IA 50014, USA

E-mail: hauptman@iastate.edu

Abstract. We have measured the neutron fraction event-by-event in beam test data taken at CERN by the DREAM collaboration. I will review these measurements in the context of the importance of neutrons to future high-precision calorimetry, and bring together the data from SPACAL , the GLD compensating calorimeter, and DREAM to estimate the impact neutron fraction measurements will make on hadronic energy resolution in dual-readout calorimeters.

Introduction: compensation and dual-readout ("dynamic compensation")

After reviewing the history of compensating calorimetry in SPACAL and the GLD concept calorimeter, I will describe the benefits of neutron measurements in dual-readout calorimetry, both integral to the DREAM module and separately in "leakage counters".

The measurement of the slow neutrons from nuclear break-up in hadronic showers is one means of achieving compensation, that is, the equality of the mean electromagnetic (e) and hadronic (h) response of a hadron-induced shower, often referred to as "$e/h = 1$". This was first demonstrated in the SPACAL test module [1], and later in the ZEUS calorimeter tests, and again in the GLD test module [2]. However, this compensation required a specific ratio of absorber (Pb) to sensor (plastic scintillator) of approximately 4-to-1 by volume, which in turn limited the electromagnetic energy resolution due to the small scintillator sampling fraction. Dual-readout calorimetry was invented [3] to solve this problem: achieve compensation with almost *any ratio* of absorber to sensor, and for almost *any absorber* and *any dual sensors*. This flexibility in achieving compensation is made possible with dual-readout calorimeters.

1. SPACAL compensating calorimeter

Neutrons liberated from broken-up nuclei will have kinetic energies, T, in the MeV region from their nuclear Fermi motion, corresponding to velocities of $v \sim \sqrt{2T/M_n} \sim 0.04c \sim 1$ cm/ns, and will

[1] DREAM collaboration (2010): N. Akchurin[a], F. Bedeschi[b], A. Cardini[c], R. Carosi[b], G. Ciapetti[d], R. Ferrari[e], S. Franchino[f], M. Fraternali[f], G. Gaudio[e], J. Hauptman[g], M. Incagli[b], F. Lacava[d], L. La Rotonda[h], S. Lee[g], M. Livan[f], E. Meoni[h], A. Negri[f], D. Pinci[d], A. Policicchio[h], S. Popescu[a], F. Scuri[b], A. Sill[a], G. Susinno[h], W. Vandelli[i], T. Venturelli[h], C. Voena[d], I. Volobouev[a], and R. Wigmans[a],

[a]Texas Tech University, Lubbock (TX), USA; [b]Dipartimento di Fisica, Università di Pisa and INFN Sezione di Pisa, Italy; [c]Dipartimento di Fisica, Università di Cagliari and INFN Sezione di Cagliari, Italy; [d]Dipartimento di Fisica, Università di Roma"La Sapienz" and INFN Sezione di Roma, Italy; [e]INFN Sezione di Pavia, Italy; [f]INFN Sezione di Pavia and Dipartimento di Fisica Nucleare e Teorica, Università di Pavia, Italy; [g]Iowa State University, Ames (IA), USA; [h]Dipartimento di Fisica, Università della Calabria and INFN Cosenza, Italy; [i]CERN, Genève, Switzerland.

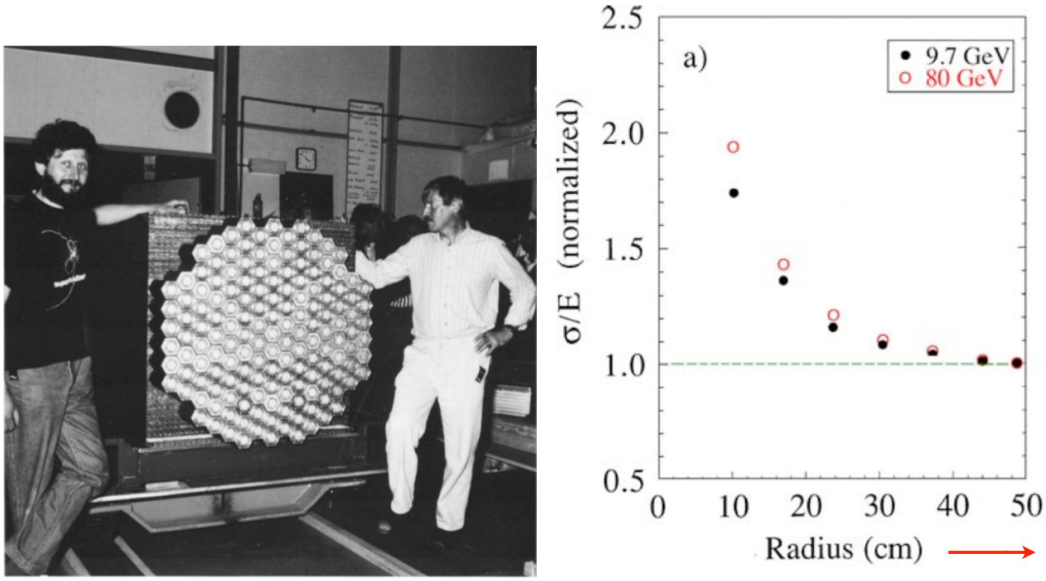

Figure 1. (a) Photograph of the compensating SPACAL module that achieved a hadronic energy resolution of nearly $30\%/\sqrt{E}$ in 9.5 $\lambda_{\rm int}$ of Pb, and with 155 channels; and, (b) the energy resolutions for hadronic showers at 9.7 and 80 GeV as a function of the volume of the calorimeter over which signals are collected. The resolution improvement is nearly a factor of 2 going from a radius of 10cm to 50cm.

therefore persist in the calorimeter volume for tens of nanoseconds as the neutrons elastically scatter from the absorber nuclei.

The protons in the H-C molecules of the scintillating fibers are the only free protons in the calorimeter. A neutron signal is generated when a neutron elastically scatters from a proton in a scintillating fiber, $np \rightarrow np$, and the recoil proton ionizes in the scintillator generating scintillation light.[2]

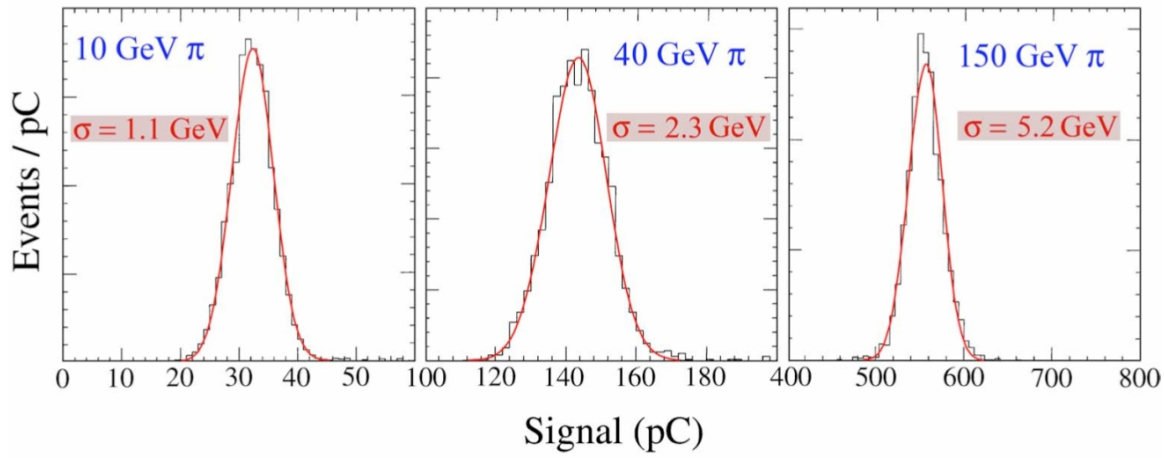

Figure 2. The direct pulse height distributions from the SPACAL module at 10, 40 and 150 GeV π^- beam energy. Distributions such as these the only honest way to correctly assess the quality of a calorimeter: the mean and width, the low side tails and the high-side tails, the linearity of the response in energy, and the degree to which the distributions are non-Gaussian. From *Nucl. Instr. Meths.* **A308** (1991) 481.

The overall energy resolution of the SPACAL module (1989, Fig. 1) is still the best ever achieved, and the pulse height response at three energies is shown in Fig. 2. These data also have a constant term similar to that found in the GLD test (Sec. 2), about 1% or less.

We emphasize that showing the full pulse height response distributions, such as those shown in Fig. 2 in units of pC, is the only honest way to correctly assess the quality of a calorimeter. Everything about these distributions is important: the mean and width, the low-side tails and the high-side tails, the linearity of the response in energy, and the degree to which the distribution is non-Gaussian.

2. GLD concept detector compensating calorimeter

The GLD ("Global Large Detector") concept detector [2] was designed for the ILC with a compensating Pb-scintillator sampling calorimeter in the ratio 8mm:2mm. This sampling is a factor of 2 coarser than the ZEUS prototype calorimeter tests and therefore one expects an electromagnetic energy resolution of $\sqrt{2} \times (\sigma_E/E)_{\rm zeus} \approx \sqrt{2} \times 18\%/\sqrt{E} \approx 25\%/\sqrt{E}$. This design was thoroughly simulated and the corresponding calorimeter module was tested from 1 to 200 GeV with e^- and π^- beams.

The time-dependence of the energy resolution for π^--induced showers simulated at 4 GeV is shown in Fig. 3(a) out to 1000 ns. The hadronic energy resolution improves from about 32% to 25% essentially due to the accumulation of the neutrons as part of the total signal, thereby reducing the overall energy fluctuations. Further plots from this simulation in Ref. [2] show a 30% increase in the total signal due to the neutrons, and the distribution of the neutron arrivals in both space and time.

Both the electromagnetic and the hadronic energy resolutions are shown in Fig. 3(b) and both demonstrate a dominant $1/\sqrt{E}$ dependence with stochastic terms of 23.9% for e^- and 46.7% for π^-. Also impressive are the small constant terms of 0.8% and 0.9% for e^- and π^-, respectively.

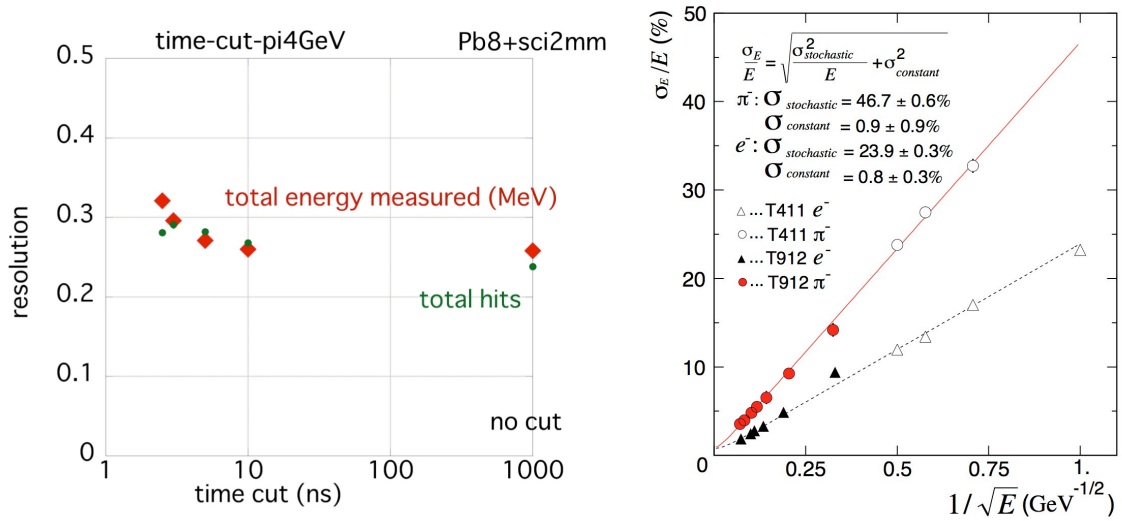

(a) (b)

Figure 3. GLD concept detector: (a) simulation showing the energy resolution as a function of an upper time cut (in ns) on the accumulated signal improving from about 32% for $t < 3$ns to 25% for $t < 1000$ns. (b) the corresponding data for both e^- and π^- beams demonstrating excellent energy resolutions and, more importantly, small constant terms of 0.9% and 0.8% for π^- and e^-, respectively.

[2] This scintillation light luminosity is suppressed by Birks recombination for densely ionizing slow protons by a factor of approximately $\sim (1 + k_B \cdot dE/dx)^{-1}$ for dE/dx in MeV/g-cm^{-2} and $k_B \approx 0.008$ g-cm^{-2}/MeV.

3. DREAM dual-readout calorimeter

The DREAM geometry used in these neutron measurements is shown in Figs. 4(a,b). Four signals are collected and recorded in the digital oscilloscope: the scintillation signals summed for the central channel (chan-1), the inner ring of 6 channels (chan-2), the outer ring of 12 channels (chan-3), and the Čerenkov signal (chan-4) summed for 16 of the 19 channels[3].

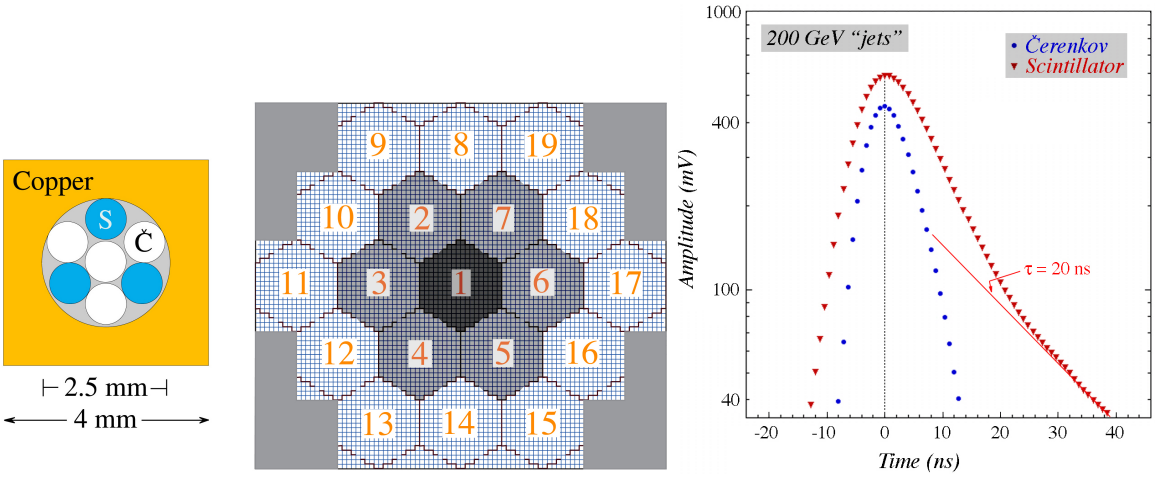

. (a) (b) (c)

Figure 4. (a) The basic building block of DREAM showing the Cu absorber and the seven fibers (3 scintillating and 4 clear); (b) the channel geometry of the module. The filling material on the periphery is Al; and, (c) the average time distribution of the Čerenkov and scintillation light for the signal summed over the whole module showing the fast Čerenkov light and the slower scintillation light with a clear neutron component with a 20ns effective lifetime inside the module.

The mean Čerenkov pulse and the mean scintillation pulse are shown in Fig. 4(c), and the neutron signal is defined as the integral under the scintillation pulse from 20 to 40 ns for each event. The distribution of this neutron signal for 200 GeV "jets"[4] divided by the total energy is called the "neutron fraction", f_n, and is shown in Fig. 5(a) plotted against the usual dual-readout electromagnetic fraction, $f_{\rm EM}$, defined in Ref. [4]. The anti-correlation between f_n and $f_{\rm EM}$ is purely physical and represents fluctuations between π^0 and $\pi^\pm$ production in hadronic shower development.[5]

The Čerenkov pulse height distribution is shown in Fig. 5(b) as broad, asymmetric and non-Gaussian. Selections on the neutron fraction, f_n, reveal that this Čerenkov distribution is a sum of narrower Gaussians also shown in Fig. 5(b). Correcting the whole distribution linearly by f_n, the original raw Čerenkov distribution results in a narrower distribution with an effective resolution (σ/μ) improvement of about 20% at all three jet energies 100, 200, and 300 GeV. This is shown in Fig. 6(a) as a function of $1/\sqrt{E}$. The f_n-corrected response has a negligible constant term as indicated by the line drawn through the origin (not a fit). In addition, the effect on the resolution due to neutrons in the leakage counters is shown in Fig. 6(b).

All of this argues strongly for the benefits of event-by-event neutron measurements in high-precision hadronic calorimetry.

The energy resolution of a hadronic calorimeter is limited by fluctuations, primarily fluctuations in $\pi^\pm$ *vs.* π^0 production, secondarily by fluctuations in the binding energy losses from broken-up

[3] The three channels left out were on the periphery of the module and chosen uniformly

[4] These are "interaction" jets generated by placing a 0.1-$\lambda_{\rm int}$ lucite block in front of DREAM and accepting events with a charged particle multiplicity above 12 exiting the lucite.

[5] There are two physical effects which suppress the mean value of f_n: the small 1 kt volume of the DREAM module and Birks suppression.

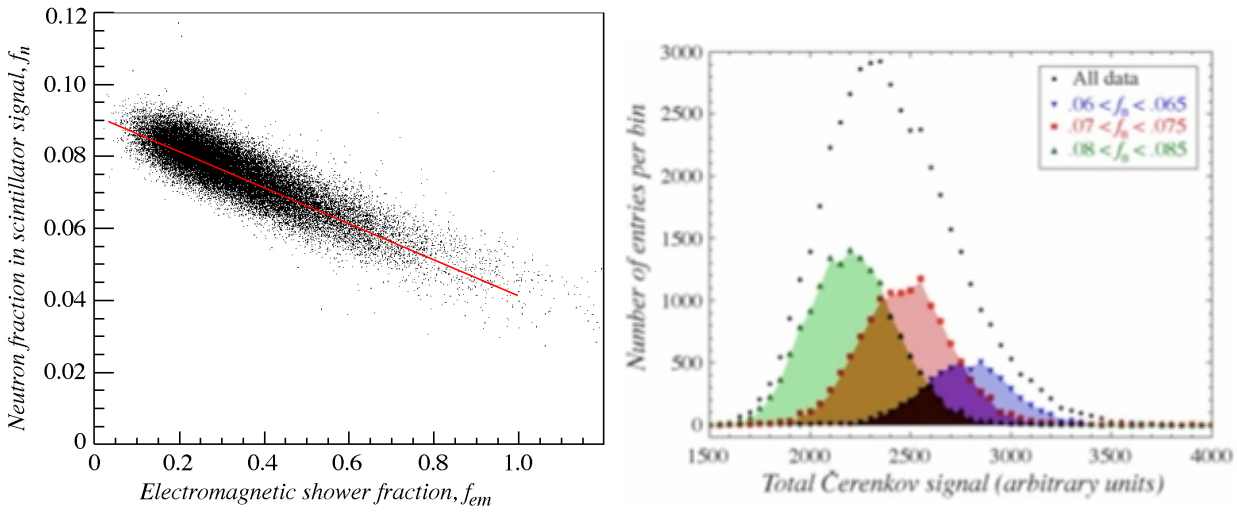

(a) (b)

Figure 5. A plot of the neutron fraction, f_n, against the electromagnetic fraction, $f_{\rm EM}$, shows their approximately linear anti-correlation and demonstrates the fundamental fluctuation between π^0 and $\pi^{\pm}$ production in hadronic interactions; and, (b) the decomposition of the full Čerenkov pulse height distribution into its Gaussian components as a function of f_n.

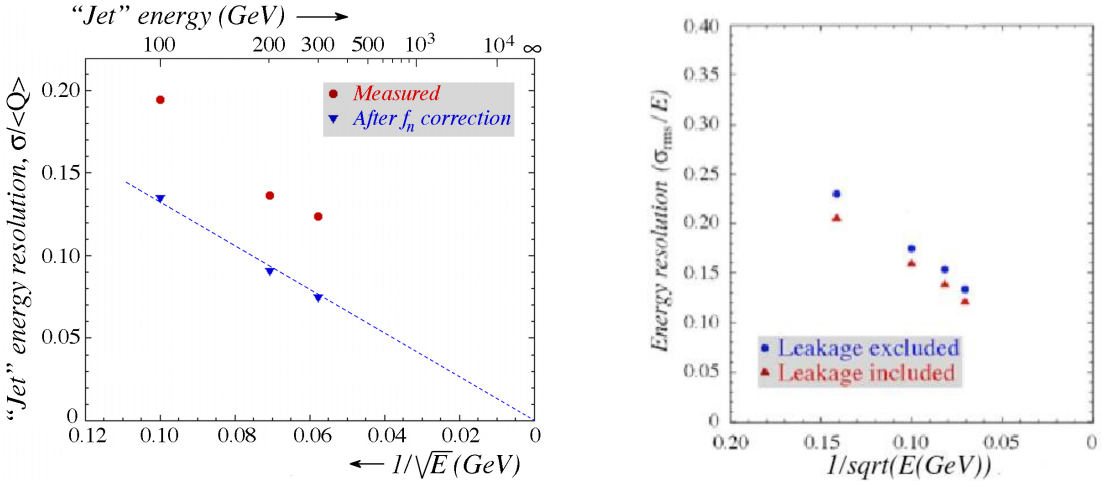

(a) (b)

Figure 6. (a) The resolution (σ/μ) of the overall raw measured Čerenkov response (upper red circles), and after linearly correcting the Čerenkov response by f_n (lower blue triangles); and, (b) the resolution with and without the addition of the neutron signals from the leakage counters.

nuclei, and thirdly, by leakage. In the DREAM module, the leakage is lateral and primarily consists of neutrons from the small module. In Fig. 7(a) we select small ranges in the electromagnetic fraction, $f_{\rm EM}$ (*e.g.*, $0.40 < Q/S < 0.42$), and look at the remaining fluctuations in the neutron fraction, f_n, plotted against the total Čerenkov signal. The f_n fluctuations are about 5%. For a slice at larger $f_{\rm EM}$ ($0.070 < Q/S < 0.75$) and therefore smaller neutron fraction, the fluctuations in f_n are about 10%. Quantitatively, for this $f_{\rm EM}$ selection and an additional selection on f_n, $0.045 < f_n < 0.065$, the distribution in total Čerenkov signal is shown in Fig. 7(b) and fitted to a Gaussian resolution of 4.7%. For a tighter selection of $0.050 < f_n < 0.055$, the fitted resolution narrows to 4.4%. This is close to the

expected fluctuations due to leakage in the DREAM module.

It is perfectly clear that the measurement of neutron energy, both internal to DREAM (Fig. 6(a)) and external (Fig. 6(b)) in the leakage counters, improves the estimate of hadronic shower energy. The theoretical lower limit of $\sigma/E \sim 15\%/\sqrt{E}$ on hadronic energy resolution [3] will be sought

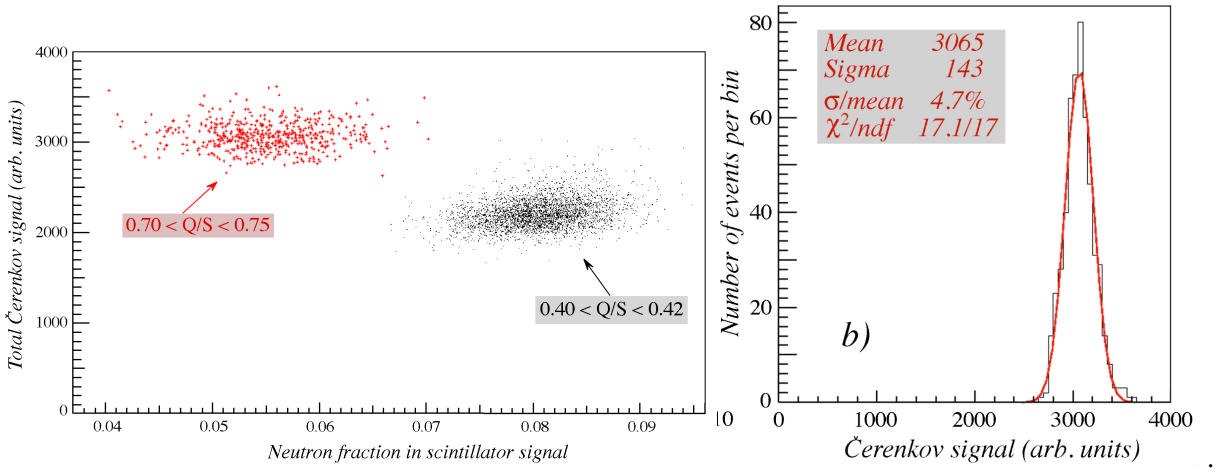

(a) (b)

Figure 7. For 200 GeV jets, (a) a scatter plot of the Čerenkov signal and the neutron fraction for two selections on the electromagnetic fraction, $f_{\rm EM}$; and, (b) the resulting resolution (σ/μ) for fixed $f_{\rm EM}$ given by $0.70 < Q/S < 0.75$ and restricted neutron content, $0.045 < f_n < 0.065$, is fitted to be 4.7%. Narrowing the f_n content to $0.050 < f_n < 0.055$ narrows the resolution distribution to 4.4%.

experimentally with a larger calorimeter of the DREAM type with expected mean leakage of about 1%. The measurements and calculations in Figs. 1(b) and 3(a) demonstrate that a large volume and long times are both required for good hadronic energy resolution that depends on the measurement of the neutrons liberated in nuclear break-up.

3.1. Acknowledgments

We acknowledge the US Department of Energy through grant DE-PS02-09ER09-02 for this work, and for its support of the original DREAM module and for continued support of these and other measurements by the DREAM collaboration. We also acknowledge the support of INFN in our plans for improving the neutron measurements. Finally, we acknowledge the excellent quality and variety of beams at CERN.

References

[1] Acosta D *et al.* 1990, *Nucl. Instr. and Meth.* **A294**, 193.
[2] Uozumi S, *et al.*, 2002, *Nucl. Instr. and Meth.* **A487**, 291.
[3] Wigmans R 2000, *Calorimetry: Energy Measurement in Particle Physics*, International Series of Monographs on Physics, Vol. 107, Oxford University Press (2000).
[4] Akchurin N *et al.* 2005, *Nucl. Instr. and Meth.* **537**, 537: "Hadron and Jet Detection in a Dual-Readout Calorimeter".